

GENETIC-ALGORITHM AND FINITE-ELEMENT APPROACH TO THE SYNTHESIS OF DISPERSION-FLATTENED FIBER

Davi Correia,¹ Vitaly F. Rodríguez-Esquerre,¹ and Hugo E. Hernández-Figueroa¹

¹ Department of Microwaves and Optics (DMO)
School of Electrical and Computer Engineering (FEEC)
University of Campinas
(UNICAMP)
13083-970 Campinas-SP, Brazil

Received 5 June 2001

ABSTRACT: A novel numerical approach for the efficient synthesis of dispersion-flattened fibers is presented. This approach is based on the combination of genetic algorithms and finite elements. Severe constraints, such as a given maximum monochromatic dispersion level and maximum flatness over a desired band, are easily attained. To show the validity and usefulness of our approach, three different profiles are optimized, and their results are compared with published ones. © 2001 John Wiley & Sons, Inc. *Microwave Opt Technol Lett* 31: 245–248, 2001.

Key words: genetic algorithm; finite elements; dispersion-flattened fiber; optimization

I. INTRODUCTION

Although single-mode optical fibers have been widely used in long transmission networks, one of their main limitation effect is the chromatic dispersion D . In order to minimize its impact on signal degradation, and consequently, on the system transmission rates [1], it is desirable that, over the operation band, the chromatic dispersion be as flat as possible, with levels kept close to, but different from zero. Several kinds of index profiles matching these requested features have been proposed [2–5], however, a general technique capable of synthesizing them in a systematic and effective way, such as the one proposed here, has not yet been reported.

Since D is proportional to the second derivative with respect to the wavelength of the effective propagation constant β , then a high accuracy of β is required. The use of the finite element method (FEM) is widely recognized as a powerful numerical tool for the analysis of microwave and optical waveguides [7]. Highly accurate finite element approaches for the computation of β , based on second-order Lagrangian [6–7] and Hermitian [8] polynomials for the one-dimensional analysis of optical fibers with arbitrary profiles have already been reported.

On the other hand, genetic algorithms (GAs) have proved to be an efficient tool to optimize electromagnetic structures, as can be realized from the vast literature available [9–11]. Most of the GA's electromagnetic applications have been focused on microwave devices and antennas; for photonics, however, very few attempts have been reported. The most attractive GA features are its robustness and capability to deal with nondifferentiable functions. This characteristic permits a substantially more flexible and simpler definition of the objective function than differentiable optimization techniques [12].

Contract grant sponsor: Brazilian Agency FAPESP
Contract grant number: Proc. 00/04371-3 and 98/16202

II. FINITE-ELEMENT MODEL

The linearly polarized modes LP_{0m} in a weakly guiding fiber with an arbitrary index profile $n(r)$ are governed by the scalar wave equation

$$\frac{\partial^2 \phi}{\partial r^2} + \frac{1}{r} \frac{\partial \phi}{\partial r} + k_0^2 [n^2(r) - \beta^2] \phi = 0 \quad (1)$$

where ϕ represents the mode electric field, β is the effective propagation constant (or also called the effective refractive index), k_0 is the wavenumber of free space, and r is defined over a truncated domain, defined by the interval $[0, a]$.

Dividing the domain $0 \leq r \leq a$ into a number of Lagrangian line elements, within each element (subinterval), ϕ is defined as $\phi = \{N\}^T \{\phi\}_e$, where the components of vector $\{\phi\}_e$ are the values of the field ϕ , defined at the corresponding nodal points, vector $\{N\}^T$ contains the shape functions, and T denotes the transpose. Using the finite-element method based on the Galerkin procedure applied to (1) leads to the following eigenvalue matrix problem:

$$[A]\{\phi\} = \beta^2 [B]\{\phi\} \quad (2)$$

where $[A]$ and $[B]$ are matrices given in [7]. Equation (2) is solved by the subspace iteration method [13]. Along this work, second-order (quadratic) Lagrangian functions were adopted [8], as a consequence, matrices $[A]$ and $[B]$ are pentadiagonals.

It is worth noting that the refractive-index profile $n(r, \lambda_0)$ of an optical fiber can be written as [2] $n(r, \lambda_0) = \eta(r, \lambda_0) \cdot n_s(\lambda_0)$, where $n_s(\lambda_0)$ is the refractive index of pure silica SiO_2 and $\eta(r, \lambda_0)$ is the normalized refractive index or the relative refractive index spatial variation. Next, assuming η to be a function of the radial coordinate only, i.e., $n(r, \lambda_0) = \eta(r) \cdot n_s(\lambda_0)$, the Sellmeier constants for the pure silica's refractive index, $n_s(\lambda_0)$, given in [4] and [14], can be taken into account, and thus, the material dispersion is directly included in our calculations.

Once β is obtained from (2) within a wavelength range, the chromatic dispersion, called simply dispersion from here on, is readily computed by using the well-known expression

$$D = -\frac{\lambda_0}{c} \frac{\partial^2 \beta}{\partial \lambda_0^2} \quad (3)$$

III. GENETIC ALGORITHM AND INDEX PROFILES

The GA adopted here follows the standard binary transformation [12], and has been successfully tested in the synthesis of Yagi antennas [15]. Thus, if x is a variable parameter of the index profile that takes real values between x_{\min} and x_{\max} , then, it is decoded as

$$x = x_{\min} + \frac{(x_{\max} - x_{\min})}{2^{N_x} - 1} \sum_{j=0}^{N_x-1} b_j^x 2^j \quad (4)$$

where the b_j^x , $j = 0, \dots, N_x - 1$ are the N_x bits describing x .

The W [4], linear chirp [3], and triangular [5] profiles were chosen to validate the present approach. The W -profile's geometry and its variable parameters are illustrated in Figure 1. We took as reference the parameters corresponding to the optimum values given in [4]. Next, we fixed $\eta_1 = 1.00$, and defined (around the reference values) the intervals shown in Table 1.

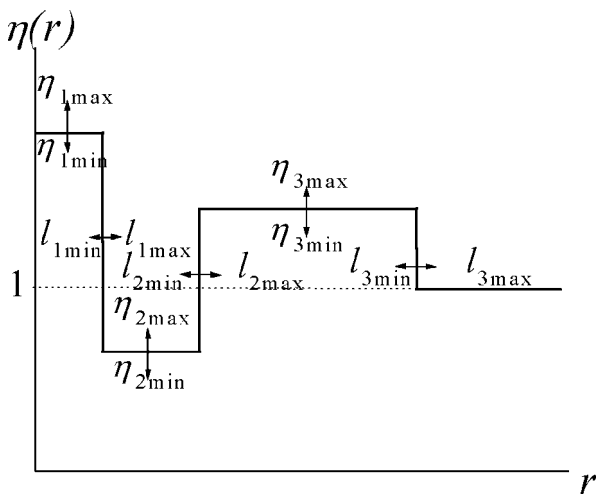


Figure 1 W profile, suggested in [4], and variable parameters

TABLE 1 Interval Limits for the Variable Parameters Related to the W -Profile in Figure 1 [4]

	η_2	η_3	η_4	l_1 (μm)	l_2 (μm)	l_3 (μm)
Max. value	0.9945	0.9990	0.9970	4.4	8.5	16.5
Min. value	0.9930	0.9975	0.9950	4.0	8.0	16.0

Following [4], the fitness or objective function was defined considering the following restrictions: find an optimum index profile such that the dispersion curve $D(\lambda)$ behaves as flat as possible over a wavelength range $I: [\lambda_{\min}, \lambda_{\max}]$, and exhibits zero values at 1.3 and 1.5 μm . Thus, the fitness function proposed for the profile p is written as follows:

$$F(p) = -|D(p, 1.3 \mu\text{m})| - |D(p, 1.5 \mu\text{m})| - \left| \sum_{\lambda=1.3 \mu\text{m}}^{\lambda=1.5 \mu\text{m}} D(p, \lambda) \right|. \quad (5)$$

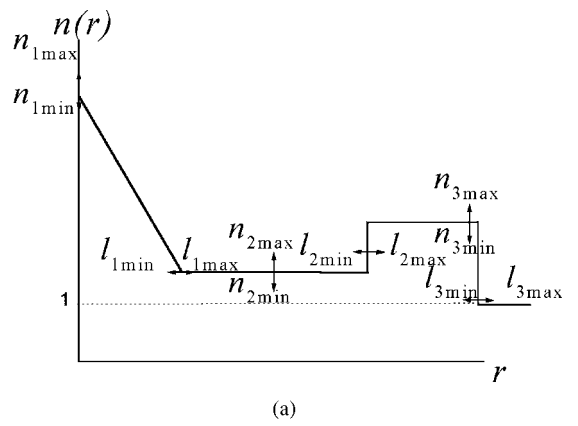
The triangular profile's geometry and its variable parameters are illustrated in Figure 2(a). We took a reference profile based on typical values given in [5]. After exhaustive attempts, it became clear that the best results are obtained with the first clad being as thin as possible. This strongly suggested that a triangular single clad [Fig. 2(b)] is enough to achieve the optimum behavior. Next, we defined (around the reference values) the variation intervals shown in Table 2.

The linear chirp profile's geometry is defined by

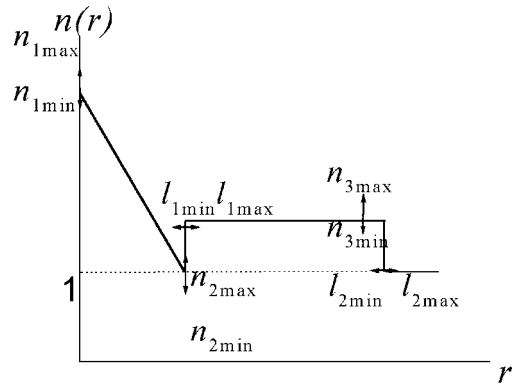
$$\eta(r) = \begin{cases} \{1 - \Delta[1 - \exp(-\alpha r) \cos(2\pi N r^2/a^2)]\}, & r \leq a \\ (1 - \Delta), & r \geq a \end{cases} \quad (6)$$

and is illustrated in Figure 3. Two different sets of values are shown, demonstrating its sensibility. As a reference, we used typical values given in [3], and as before, the variable parameters (N , Δ , α , and a) were allowed to vary around the reference values, over the intervals shown in Table 3.

The fitness function was requested to match the following restrictions: find an optimum index profile such that the dispersion curve $D(\lambda)$ behaves as flat as possible over a



(a)



(b)

Figure 2 Triangular profile, suggested in [5], and variable parameters for double (a) and single (b) clad

TABLE 2 Interval Limits for the Parameters Related to the Triangular Profile Shown in Figure 2 [5]

	η_1	η_2	η_3	l_1 (μm)	l_2 (μm)
Max. value	1.004	0.9990	1.0010	8.0	$l_1 + 5.8$
Min. value	1.003	0.9970	0.9990	7.0	$l_1 + 2.8$

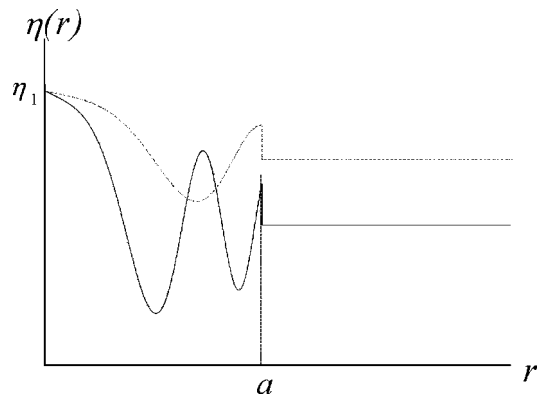


Figure 3 Two different linear chirp profiles. $N = 1.87742$, $a = 7.0 \mu\text{m}$, $\Delta = 0.01565$, $\alpha = 0.11613$ (solid curve), which correspond to optimum parameters, and reference parameters: $N = 1.0$, $a = 7.0 \mu\text{m}$, $\Delta = 0.008$, $\alpha = 0.1$ (dotted curve)

TABLE 3 Interval Limits for the Variable Parameters Related to Linear Chirp Profile Shown in Figure 3 [3]

	N	Δ	α	a (μm)
Max. value	2.0	0.015	0.2	7.5
Min. value	0.0	0.001	0.0	6.5

wavelength range $I: [\lambda_{\min}, \lambda_{\max}]$, and exhibits a maximum dispersion value D_{\max} at a given wavelength λ_0 , which belongs to I . The fitness function proposed here is given by

$$F(p) = - \left(\sum_{\lambda=\lambda_{\min}}^{\lambda=\lambda_{\max}} |D_{\max} - D(p, \lambda)| \right) - \left| \frac{\partial(D(p, \lambda_0))}{\partial \lambda} \right|. \quad (7)$$

The values $\lambda_{\min} = 1.5 \mu\text{m}$, $\lambda_{\max} = 1.6 \mu\text{m}$, $\lambda_0 = 1.55 \mu\text{m}$, and $D_{\max} = 0.2 \text{ ps/km} \cdot \text{nm}$ were adopted.

IV. NUMERICAL RESULTS

The W -profile's optimum dispersion curves obtained using the present scheme and the one described in [4] are shown in Figure 4. Our optimum dispersion curve corresponds to the values $\eta_1 = 1.00$, $\eta_2 = 0.9944$, $\eta_3 = 0.9983$, $\eta_4 = 0.9960$, $l_1 = 4.106 \mu\text{m}$, $l_2 = 8.133 \mu\text{m}$, $l_3 = 14.60 \mu\text{m}$. It is clear that the result obtained here satisfies in a better way the requested restrictions in (5). We notice that our starting point was the optimum profile reported in [4]. Therefore, our scheme improved that result both in flatness and zero chromatic dispersion at $1.3 \mu\text{m}$ and $1.55 \mu\text{m}$.

The triangular profile's optimum dispersion curves obtained using the present scheme and the one described in [5] are shown in Figure 5. Our optimum dispersion curve corresponds to the values $\eta_1 = 1.00343$, $\eta_2 = 0.99778$, $\eta_3 = 1.00007$, $l_1 = 7.600 \mu\text{m}$, and $l_2 = 12.147 \mu\text{m}$. The result clearly satisfies the restrictions imposed by (7).

The optimum dispersion curves for the linear chirp profile are shown in Figure 6. Here, our optimum parameters are $a = 7.0 \mu\text{m}$, $\Delta = 0.01565$, $\alpha = 0.11613$, and $N = 1.87742$. Unfortunately, the results obtained in [3] seem to be inaccurate. The optimum curve shown in [3] is similar to our optimum one shown in Figure 3. However, plugging the optimum parameters given in [3] into our direct code, what

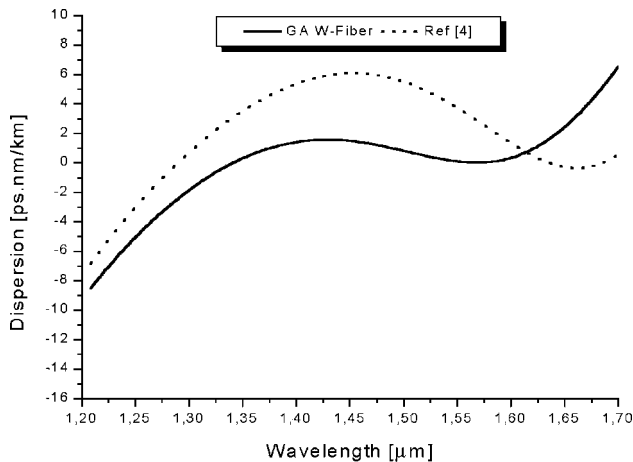


Figure 4 W -profile dispersion curves: optimum, using the present algorithm (solid), and reference parameters taken from [4] (dotted)

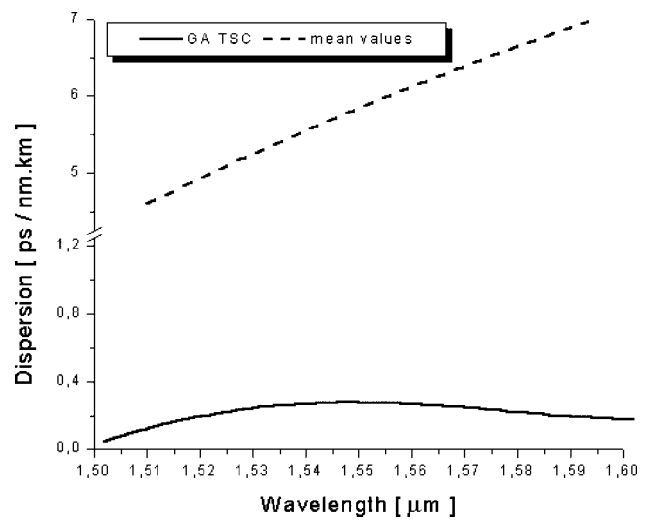


Figure 5 Triangular single-clad profile dispersion curves: optimum, using the present algorithm (solid), and reference or intervals mean parameters (dashed)

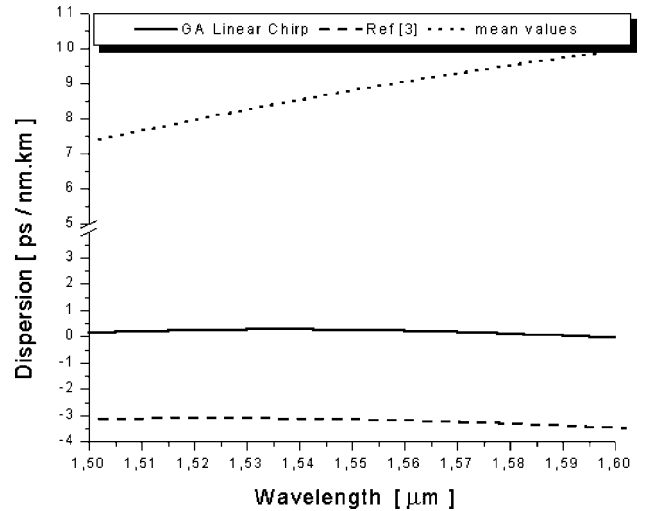


Figure 6 Linear chirp profile dispersion curves: optimum, using the present algorithm (solid), reference or interval mean parameters (dotted), and convergent solution for optimum parameters found in [3] (dashed)

we, in fact, obtained, after reaching convergence, is the dashed curve shown in Figure 3. On the other hand, the optimum profile reported in [3] was obtained by mapping D_{\max} versus only α and N , and not through a systematic and general optimization approach as shown here.

V. CONCLUSIONS

In this work, we have proposed a new approach for the synthesis of dispersion-flattened index profiles. This approach combines the GA for optimization and the FEM as a numerical tool for the direct calculation of monochromatic dispersion curves. The results obtained for the three profiles analyzed here show the usefulness and competitiveness of this approach. The optimum profiles were obtained after a moderate amount of computer time: around 40 min using a SUN ULTRA 5 station, 250 MHz, HD 4.3 Gbytes, and 128 Mbytes RAM.

REFERENCES

1. T. Okuno, M. Onishi and M. Nishimura, Generation of ultra-broad-band supercontinuum by dispersion-flattened and decreasing fiber, *IEEE Photon Technol Lett* 10, (1998), 72–74.
2. R. Lundin, Minimization of chromatic dispersion over a broad wavelength in a single-mode optical fiber, *Appl Opt* 32 (1993), 3241–3245.
3. S.P. Survaiya and R.K. Shevgaonkar, Dispersion characteristics of an optical fiber having linear chirp refractive index profile, *J Lightwave Technol* 17, (1999), 1797–1805.
4. H. Eitzkorn and W.E. Heinlein, Low-dispersion single-mode silica fiber with undoped core and three F-doped cladding, *Electron Lett* 20 (1984), 423–424.
5. K.B. Chung and S.S. Choi, Propagation characteristics of a triangular-index doubly clad monomode fiber, *Electron Lett* 21 (1985), 271–273.
6. M. Koshiya, *Optical waveguide theory by the finite element method*, KTC Scientific Publishers, 1992.
7. Q.-Y. Li, Propagation characteristics of single mode optical fibers with arbitrary refractive-index profile: The finite quadratic element approach, *J Lightwave Technol* 9 (1991), 22–26.
8. V.F. Rodríguez-Esquerre and H.E. Hernández-Figueroa, Hermitian finite element approach for optical fiber dispersion analysis, *Proc SBMO/IEEE, MTT-S, AP-S, and LEOS Int Microwave and Optoelectron Conf, IMOC'99, Rio de Janeiro, Brazil, Aug. 1999*, pp. 198–201.
9. D.S. Weile and E. Michielssen, Genetic algorithm optimization applied to electromagnetics: A review, *IEEE Trans Antennas Propagat* 45 (1997), 343–353.
10. R.L. Haupt, An introduction to genetic algorithm for electromagnetics, *IEEE Trans Antennas Propagat Mag* 37 (1995), 7–15.
11. Y. Rahmat-Samii and E. Michielssen, *Electromagnetic optimization by genetic algorithm*, Wiley, New York, 1999.
12. D. Goldberg, *Genetic algorithm in search, optimization & machine learning*, Addison-Wesley Longman, Reading, MA, 1989.
13. B.N. Parlet, *The symmetric eigenvalue problem*, Prentice-Hall, Englewood Cliffs, NJ, 1980.
14. J.W. Fleming, Material dispersion in lightguide glasses, *Electron Lett* 14 (1978), 326–328.
15. D. Correia, A.J.M. Soares, and M.A.B. Terada, Optimization of gain, impedance and bandwidth in Yagi-Uda antennas using genetic algorithms, *Proc SBMO/IEEE, MTT-S, AP-S, and LEOS Int Microwave and Optoelectron Conf, IMOC'99, Rio de Janeiro, Brazil, Aug. 1999*, pp. 41–44.

© 2001 John Wiley & Sons, Inc.

A COMPARISON BETWEEN TWO HYBRID TECHNIQUES FOR THE SCATTERING FROM FINITE FREQUENCY-SELECTIVE SURFACES

C. Pochini,¹ G. Toso,² G. Pelosi,¹ and A. Roederer²

¹Dipartimento di Elettronica e Telecomunicazioni
Università di Firenze
I50134 Florence, Italy

²Antenna Section
Electromagnetics Division
European Space Research and Technology Centre, ESA ESTEC
2201 AG Noordwijk, The Netherlands

Received 11 June 2001

ABSTRACT: *The scattering from finite frequency selective surfaces (FSSs) characterized by planar interfaces is analyzed, resorting to two PO-based hybrid techniques. The hybrid techniques, validated with a full-wave numerical technique, are easy to implement, fast, and already*

quite accurate for medium-size FSSs. © 2001 John Wiley & Sons, Inc. *Microwave Opt Technol Lett* 31: 248–252, 2001.

Key words: *frequency-selective surfaces (FSSs); scattering; hybrid techniques*

1. INTRODUCTION

In this paper, the scattering from finite frequency-selective surfaces (FSSs) characterized by planar interfaces is analyzed, resorting to two PO-based hybrid techniques. FSSs are periodic structures exhibiting specific filtering properties with respect to the frequency. The optimization of their electrical characteristics allows one to design high-performance multi-band and/or broadband antenna systems. Several numerical techniques have been successfully implemented to characterize the electromagnetic behavior of infinite FSSs [1–3]. For this kind of analysis, it is sufficient to consider the elementary cell of the FSS and the imposition of the periodicity conditions on the lateral walls of the cell itself. Due to their finite dimensions, the properties of real FSSs can significantly differ from the ones relevant to the corresponding infinite FSSs. To account for the finite dimensions of FSSs, several strategies recently have been adopted; see, for instance, [4–11]. For most applications, FSS structures are too large, in terms of wavelengths, for a full-wave rigorous analysis to be implemented. That is the reason why approximate techniques are normally implemented for finite FSSs.

The most efficient solutions proposed to describe finite FSSs are hybrid techniques combining numerical techniques and high-frequency techniques. In [4], for instance, a PO-based technique has been implemented to analyze the plane-wave scattering from a finite array of metallic waveguides. In [7], a heuristic uniform geometrical theory of diffraction (UTD) solution for plane-wave scattering from edges in periodic planar surfaces has been proposed and successfully compared with a full-wave solution. In [9], the physical-optics (PO) technique has been used together with a finite element method (FEM) to study the electromagnetic field scattered from finite periodic structures. Independently of the high-frequency technique chosen, the starting point in the implementation of these hybrid techniques, is always the characterization, via a rigorous numerical technique, of the corresponding infinite FSS structure.

An alternative hybrid procedure, recently presented [11], is based on commercial electromagnetic solvers not devoted to the analysis of infinite periodic structures, like the method-of-moments (MoM)-based FEKO [12]. These commercial tools are efficient in the electromagnetic modeling of finite FSSs limited to a maximum size determined by the capabilities of the work station used. To model, using these commercial solvers, finite FSSs with dimensions exceeding this maximum size, we extract from the assigned FSS structure a finite portion. The scattered field, relevant to this reduced-size FSS, sampled along the near field cuts chosen in such a way that the diffraction effects can be neglected on them, can be approximated with the field relevant to the corresponding infinite FSS. By imposing that this field is expressed in a Floquet mode expansion, an estimation of the Floquet mode amplitudes characterizing the corresponding infinite FSS structure is obtained. Finally, resorting to a standard uniform asymptotic physical-optics (UAPO) procedure, the electromagnetic field associated with the initial FSS structure can be estimated. Once the hybrid approach is implemented, it is quite simple to modify the structure and perform a new